NASA/TM–2011-216883

Refined Exploration of Turbofan Design Options for an Advanced Single-Aisle Transport

Mark D. Guynn
Langley Research Center, Hampton, Virginia

Jeffrey J. Berton, Kenneth L. Fisher, William J. Haller, and Michael T. Tong
Glenn Research Center, Cleveland, Ohio

Douglas R. Thurman
Army Research Laboratory, Cleveland, Ohio

January 2011

NASA STI Program . . . in Profile

Since its founding, NASA has been dedicated to the advancement of aeronautics and space science. The NASA scientific and technical information (STI) program plays a key part in helping NASA maintain this important role.

The NASA STI program operates under the auspices of the Agency Chief Information Officer. It collects, organizes, provides for archiving, and disseminates NASA's STI. The NASA STI program provides access to the NASA Aeronautics and Space Database and its public interface, the NASA Technical Report Server, thus providing one of the largest collections of aeronautical and space science STI in the world. Results are published in both non-NASA channels and by NASA in the NASA STI Report Series, which includes the following report types:

- TECHNICAL PUBLICATION. Reports of completed research or a major significant phase of research that present the results of NASA programs and include extensive data or theoretical analysis. Includes compilations of significant scientific and technical data and information deemed to be of continuing reference value. NASA counterpart of peer-reviewed formal professional papers, but having less stringent limitations on manuscript length and extent of graphic presentations.

- TECHNICAL MEMORANDUM. Scientific and technical findings that are preliminary or of specialized interest, e.g., quick release reports, working papers, and bibliographies that contain minimal annotation. Does not contain extensive analysis.

- CONTRACTOR REPORT. Scientific and technical findings by NASA-sponsored contractors and grantees.

- CONFERENCE PUBLICATION. Collected papers from scientific and technical conferences, symposia, seminars, or other meetings sponsored or co-sponsored by NASA.

- SPECIAL PUBLICATION. Scientific, technical, or historical information from NASA programs, projects, and missions, often concerned with subjects having substantial public interest.

- TECHNICAL TRANSLATION. English-language translations of foreign scientific and technical material pertinent to NASA's mission.

Specialized services also include creating custom thesauri, building customized databases, and organizing and publishing research results.

For more information about the NASA STI program, see the following:

- Access the NASA STI program home page at *http://www.sti.nasa.gov*

- E-mail your question via the Internet to help@sti.nasa.gov

- Fax your question to the NASA STI Help Desk at 443-757-5803

- Phone the NASA STI Help Desk at 443-757-5802

- Write to:
  NASA STI Help Desk
  NASA Center for AeroSpace Information
  7115 Standard Drive
  Hanover, MD 21076-1320

NASA/TM–2011-216883

Refined Exploration of Turbofan Design Options for an Advanced Single-Aisle Transport

Mark D. Guynn
Langley Research Center, Hampton, Virginia

Jeffrey J. Berton, Kenneth L. Fisher, William J. Haller, and Michael T. Tong
Glenn Research Center, Cleveland, Ohio

Douglas R. Thurman
Army Research Laboratory, Cleveland, Ohio

National Aeronautics and
Space Administration

Langley Research Center
Hampton, Virginia 23681-2199

January 2011

Acknowledgments

The authors would like to thank the Subsonic Fixed Wing Project of NASA's Fundamental Aeronautics Program for supporting this study.

Available from:

NASA Center for AeroSpace Information
7115 Standard Drive
Hanover, MD 21076-1320
443-757-5802

Contents

List of Tables

List of Figures

List of Acronyms, Symbols, and Abbreviations

ADP – Aerodynamic Design Point

ANOPP – Aircraft Noise Prediction Program

ASAT – Advanced Single-Aisle Transport

BPR – Bypass Ratio

CAEP – Committee on Aviation Environmental Protection

EIS – Entry-Into-Service

EPNL – Effective Perceived Noise Level

FAR – Federal Aviation Regulations

FLOPS – Flight Optimization System

FPR – Fan Pressure Ratio

HPC – High Pressure Compressor

HPT – High Pressure Turbine

ICAO – International Civil Aviation Organization

ISA – International Standard Atmosphere

LPC – Low Pressure Compressor

LPT – Low Pressure Turbine

LTO – Landing-Takeoff Cycle

NPSS – Numerical Propulsion System Simulation

OPR – Overall Pressure Ratio

PDCYL – Point Design of Cylindrical-Bodied Aircraft

TOC – Top-Of-Climb

TSFC – Thrust Specific Fuel Consumption

UHB – Ultra-High Bypass Ratio

WATE – Weight Analysis of Turbine Engines

Abstract

The desire for higher engine efficiency has resulted in the evolution of aircraft gas turbine engines from turbojets, to low bypass ratio, first generation turbofans, to today's high bypass ratio turbofans. It is possible that future designs will continue this trend, leading to very-high or ultra-high bypass ratio engines. A comprehensive exploration of the turbofan engine design space for an advanced technology single-aisle transport (737/A320 class aircraft) was conducted previously by the authors and is documented in a prior report. Through the course of that study and in a subsequent evaluation of the approach and results, a number of enhancements to the engine design ground rules and assumptions were identified. A follow-on effort was initiated to investigate the impacts of these changes on the original study results. The fundamental conclusions of the prior study were found to still be valid with the revised engine designs. The most significant impact of the design changes was a reduction in the aircraft weight and block fuel penalties incurred with low fan pressure ratio, ultra-high bypass ratio designs. This enables lower noise levels to be pursued (through lower fan pressure ratio) with minor negative impacts on aircraft weight and fuel efficiency. Regardless of the engine design selected, the results of this study indicate the potential for the advanced aircraft to realize substantial improvements in fuel efficiency, emissions, and noise compared to the current vehicles in this size class.

1.0 Introduction

As aircraft manufacturers Boeing and Airbus continue to develop and mature new twin-aisle, wide body aircraft designs in the 210-350 seat class, for scheduled first deliveries in 2011 and 2013 respectively, significant attention is also being paid to the potential for future new products in the smaller Boeing 737/Airbus A320 class. Options under consideration include taking advantage of evolving propulsion advances through a re-engining program in the fairly near term, to development of a completely new vehicle in the farther term. Airbus has chosen to initially pursue the near term benefits of re-engining, while Boeing continues to evaluate its options (ref. 1). Regardless of the path chosen, the fuel consumption and operating cost reductions necessary to make a new product economically viable will require substantial improvements in propulsion system efficiency. It is well known in aircraft propulsion system design that it is more efficient to generate thrust by accelerating a large mass of air a small amount than by accelerating a small mass of air a large amount; propulsive efficiency increases as the ratio of exhaust velocity to free stream velocity decreases. For a turbofan engine, this can be accomplished by reducing the fan pressure ratio (FPR), which decreases the amount of fan air stream acceleration, and increasing the fan mass flow (fan size) to maintain thrust. An increase in fan mass flow for a given core engine size leads to higher bypass ratio (BPR). The desire for higher engine efficiency has resulted in the evolution of aircraft gas turbine engines from turbojets (BPR=0), to low bypass ratio, first generation turbofans (BPR=1-2), to today's high bypass ratio turbofans (BPR=5-10). It is possible that future designs will continue this trend, leading to very-high or ultra-high bypass ratio (UHB) engines. Reduced FPR has complementary benefits in lower engine noise due to the strong relationship between noise and the velocity of the air exiting the engine. Low pressure ratio fans also typically require lower tip speeds which can result in lower fan noise. Although there are fundamental noise and efficiency benefits to lowering FPR, there are typically weight and drag penalties which can potentially offset those benefits.

In addition, the larger fan diameter associated with lower FPR can lead to engine-airframe integration issues. Only through analysis of the complete aircraft system can the best FPR for a given aircraft design be determined.

Reference 2 describes a previous study conducted by the authors of this report in which the turbofan design trade space for an advanced single-aisle transport* (ASAT) was explored to investigate the impact of FPR and other engine design choices. The study was conducted to support the "N+1" goals of NASA's Subsonic Fixed Wing Project (see Figure 1) by identifying the engine designs which provide the best opportunity to meet the goals for the N+1 timeframe. ("N" refers to the current generation of aircraft flying today, "N+1" the next generation, "N+2" the second generation, and so forth.) The performance, noise, and emission characteristics of 48 different advanced engine/airframe combinations were evaluated and compared in reference 2. In developing the engines for that study, considerable attention was paid to ensuring consistent assumptions and ground rules were applied to all the engine models. However, when the assumptions and ground rules were subjected to additional scrutiny through consultation with engine manufacturers, it was determined that because of the wide breadth of engine architectures and cycle parameters encompassed by the study, the "same ground rules across all engines" approach used previously was not always appropriate. A new set of modeling assumptions and ground rules was developed to better reflect the unique characteristics of the individual engines, and a subset of the original cases (12) was re-analyzed. This report presents the results of this new analysis and comparisons to the results of the original study documented in reference 2.

CORNERS OF THE TRADE SPACE	N+1 (2015)*** Technology Benefits Relative to a Single Aisle Reference Configuration	N+2 (2020)*** Technology Benefits Relative to a Large Twin Aisle Reference Configuration	N+3 (2025)*** Technology Benefits
Noise (cum below Stage 4)	- 32 dB	- 42 dB	- 71 dB
LTO NOx Emissions (below CAEP 6)	-60%	-75%	better than -75%
Performance: Aircraft Fuel Burn	-33%**	-50%**	better than -70%
Performance: Field Length	-33%	-50%	exploit metroplex* concepts

*** Technology Readiness Level for key technologies = 4-6
** Additional gains may be possible through operational improvements
* Concepts that enable optimal use of runways at multiple airports within the metropolitan areas

Figure 1. NASA Subsonic Fixed Wing Project's system level metrics and goals.

2.0 Study Objectives and Approach

The primary objective of this study was to determine the impact of refinements to the engine design ground rules and assumptions used in reference 2 on the overall conclusions of that study. The basic analysis approach described in that report was retained; a series of analytical engine models were

* "Single-Aisle Transport" is a common way to refer to a 737/A320 class airplane; although there are other types of single-aisle aircraft (e.g., regional jets). Even though it is possible that the future 737/A320 replacements designed by Boeing and Airbus will not have single-aisle passenger layouts, the term "single-aisle transport" will be used in this report to refer to a 737/A320 class airplane.

developed and applied to a common airframe model to assess the overall performance and noise characteristics. As in the prior study, the primary engine design parameter of interest was fan pressure ratio, which is directly related to bypass ratio. In addition, the impacts of fan drive approach (direct drive vs. geared) and compression work split (between the low pressure compressor (LPC) and high pressure compressor (HPC)) were investigated. Because the results of reference 2 showed that cruise Mach number and engine overall pressure ratio (OPR) did not significantly impact the relative trends with fan pressure ratio, those parameters were not varied in the current study.

3.0 Modeling and Analysis Methodology

3.1 Propulsion System Modeling

The same propulsion system modeling tools were used for this study as in the prior work of reference 2. Cycle analysis for the engines was performed with the NPSS (Numerical Propulsion System Simulation) code (refs. 3-5). Analysis of the aeromechanical characteristics and estimates of the engine weight (including fan gearbox if applicable) were performed with the WATE (Weight Analysis of Turbine Engines) code (refs. 6-8). Estimates for engine NO_X emission indices (grams of NO_X emitted from the engine per kilogram of fuel consumed by the engine) were obtained from a correlation developed by NASA combustor technologists during the latter stages of NASA's Ultra-Efficient Engine Technology Program. Reference 2 provides more details on this empirical NO_X correlation.

All engines in the study are two-spool, separate flow, turbofans designed with the same Aerodynamic Design Point (ADP) and same OPR at the ADP. The ADP of 5,000 lb of thrust at Mach 0.8 and 35,000 ft was selected to represent a nominal top-of-climb (TOC) condition for the advanced technology airframe. The ADP engine OPR of 42 is equivalent to the "Spiral 2" analysis in reference 2. Although the OPR is the same for all the engines, two different compressor work splits were considered. The "low work" engines have a lower pressure rise across the LPC (and a higher pressure rise across the HPC) compared to the "high work" engines. Inlet mass flow for each engine was selected to achieve the net thrust requirement at ADP. The BPR was set by a jet velocity ratio (V_{core}/V_{bypass}) of 1.6 at the design point. This differs from the prior work in which an extraction ratio of 1.25 (ratio of total pressures for bypass nozzle and core nozzle) was used to set BPR. In the prior study, design point burner fuel-to-air ratio was adjusted to achieve a sea-level static (SLS) target thrust of 23,000 lb (hot day, ISA+27°F) for all of the engines. Because of the wide variation in FPR and therefore thrust lapse rates, designing to equal SLS thrust did not provide equivalent takeoff performance for all the engines. For the current study, the engines were instead designed for equal thrust at a rolling takeoff condition (sea-level, Mach 0.25). The sea-level, Mach 0.25 thrust target was set to 17,500 lb based on the takeoff thrust required for a nominal configuration. Low FPR engine cycles generally require some type of variable geometry for proper operation across the flight envelope. Two approaches commonly considered are variable pitch fan blades or a variable area fan exhaust nozzle. Because variable pitch fan blades present additional technological challenges, the use of a variable area nozzle was examined in this study. A variable area nozzle was applied when necessary to achieve the desired 20% fan surge margin throughout the operating envelope. The variable area nozzle was assessed an estimated weight penalty of 10% compared to an equivalent fixed-area design.

In the prior analysis duct pressure loss assumptions were constant across all the engines. But because of the large variation in geometry and flow conditions for the different engines, some variation in duct losses should be expected. In the current study the assumed bypass duct pressure loss was changed from a constant value to a function of FPR, with higher FPR engines having higher assumed bypass duct pressure losses due to the higher speed bypass duct flow. Another difference among the engine designs requiring consideration was the different turbine geometries of the direct drive and geared engines. The turbines of the direct drive engines have larger radial variation, which should lead to higher inter-turbine duct pressure losses. This difference in inter-turbine duct losses was added in the revised engine modeling. The low pressure turbine (LPT) cooling philosophy is another area in which refinements were made. In the previous study, a maximum LPT rotor inlet temperature of 2460°R was used to allow the LPT to be uncooled with the use of advanced, high-temperature materials. However, in the high work engines, less work is done by the high-spool, leading to higher high pressure turbine (HPT) exit temperatures, and more cooling is required to meet a 2460°R LPT rotor inlet temperature limit. The constraint of an uncooled LPT was removed for the current study and a cooling analysis was performed for each engine to determine the amount of cooling air necessary to maintain acceptable HPT and LPT temperatures. The introduction of different cooling levels for the LPT also made the prior assumption of equal LPT adiabatic efficiency across all the engines invalid. For this study LPT efficiency was varied as a function of cooling level. A minor change to the engine designs was the assumption of a two stage HPT rather than the single stage assumed previously. The two stage design was felt to be more representative of likely industry designs (ref. 9), although this change had little impact on the engine weight and performance characteristics.

Key differences between the engine design ground rules and assumptions of the current analysis and those in reference 2 are summarized in Table 1.

Table 1. Revised Engine Design Ground Rules and Assumptions

	Modeling in Reference 2	**Current Study**
Engine Thrust Sizing	ADP: 5,000 lb SLS: 23,000 lb	ADP: 5,000 lb SL, M=0.25: 17,500 lb
Bypass Ratio	Extraction Ratio of 1.25 at ADP	Jet Velocity Ratio of 1.6 at ADP
Bypass Duct Losses	Constant	Function of FPR
Inter-turbine Duct Losses	Constant	Different assumptions for direct drive and geared fan architectures
Turbine Cooling Philosophy	LPT temperature limited to allow uncooled LPT	LPT cooling permitted
LPT Adiabatic Efficiency	Constant with constant LPT loading	Function of LPT cooling level
HPT Design	Single stage	Two stage

3.2 Aircraft Sizing Analysis

As in the prior study, the study engines were combined with an advanced technology, single-aisle commercial transport airframe model to determine overall system level performance. The advanced technology, "ASAT" airframe model is a derivative of a 737-800 like baseline model intended to be representative of a potential advanced technology replacement aircraft. The aircraft sizing and synthesis computer code FLOPS (Flight Optimization System) (ref. 10) was used as the primary aircraft level sizing and analysis tool. Special sizing considerations introduced by large diameter engines were addressed through simplifying assumptions and enhancements to the FLOPS analysis. Spreadsheet analyses were used to determine landing gear length, engine-out drag, and vertical tail size so that the impacts of large diameter engines could be properly captured. Enhancements to basic FLOPS capabilities were also made in the structural weight and aerodynamics areas. The wing and fuselage structural weight estimates of FLOPS were replaced with estimates from PDCYL (ref. 11). PDCYL offers a less empirical, more analytical weight estimation methodology that is more sensitive to parameters such as engine weight and location. FLOPS aerodynamic predictions were enhanced through a model calibration process incorporating details of the 737-800 high speed and low speed aerodynamic performance. The primary airframe technology advancement assumed was extensive use of composite materials for the airframe structure. For the Boeing 787 currently in development, as much as 50% of the primary structure is made of composite materials (ref. 12). Other minor technology improvements based on the 787 included an increase in hydraulic system pressure and a slight drag reduction. Changes were also made to the design mission to reflect projected performance enhancements desired for an advanced aircraft in this vehicle class. Cruise Mach was increased slightly to 0.8 (typical cruise Mach for the 737-800 is 0.785 (ref. 13)) and design range (with 32,400 lb payload) was increased from 3060 nm to 3250 nm. Other than a slight increase in wing sweep reflecting the higher cruise Mach number, the basic 737-800 geometry was not changed for the advanced technology, ASAT model. Further details of the airframe model development and calibration process are given in reference 2.

3.3 Noise Analysis

The same noise analysis methodology and tools described in reference 2 were used in the current effort. The primary tools used for the noise analysis included: NPSS for the engine cycle analysis; WATE for the engine aeromechanical and flowpath analysis; FLOPS for the aircraft trajectory simulation; and ANOPP (Aircraft Noise Prediction Program) Level 26 (refs. 14, 15) for the source noise prediction and propagation. The NPSS and WATE codes were used to generate input data necessary for the ANOPP source noise modeling. Adjustments representing noise reduction technologies (discussed below) were made to the source noise spectra prior to propagation. ANOPP noise propagation modeling included spherical spreading, atmospheric attenuation, ground effects, reflections, and lateral attenuation. The Effective Perceived Noise Level (EPNL) was calculated at the noise certification points defined in FAR Part 36 (ref. 16). EPNL is an integration of the ground observer perceived noise time history which depends on aircraft trajectory, noise spectra propagation, frequency integration, and tonal content and amplitude penalties. Validation of the noise analysis methodology using 737-800 certification data is described in reference 2.

The same series of advanced noise reduction technologies were assumed as in the previous study. Chevrons were applied to all core nozzles and to all fixed-area bypass nozzles. Chevrons were not applied to variable area bypass nozzles due to potential conflict with the variable area nozzle design. Jet noise benefits of the nozzle chevrons were determined analytically using the 2004 Stone jet noise prediction method in ANOPP (ref. 17). This method is based on 1997 acoustic measurements of chevron-equipped nozzles from NASA Glenn's Aeroacoustic Propulsion Laboratory's Nozzle Acoustic Test Rig freejet facility (ref. 18). Conventional inlet, interstage, and aft fan duct liners were applied to reduce fan inlet and discharge noise. The benefits of these liners were modeled by applying an acoustic suppression "map" of 1/3rd octave band sound pressure level decrements to the hardwall fan source spectra predicted by ANOPP. The liner suppression map was based on measured acoustic data of 22-inch diameter fan test articles in NASA Glenn's 9×15 Low Speed Wind Tunnel (ref. 19). In addition to conventional liners, two advanced technologies were applied for fan noise reduction; soft vane stators and over-the-rotor foam metal treatment (refs. 20, 21). Both of these technologies are applications of acoustic treatment in areas of the engine which currently do not have treatment, the fan vanes and above the fan rotor tips. Acoustic tests of both of these technologies were conducted at NASA Glenn in 2008. Airframe noise reduction technologies assumed included innovative slat cove designs, flap porous tips, and landing gear fairings. These technologies are considered mature enough to be commensurate with the "N+1" timeframe.

4.0 Study Engine Designs

4.1 Engine Trade Space

The engine design trade space investigated is summarized in Table 2. ADP fan pressure ratios of 1.4, 1.5, 1.6, and 1.7 were investigated for the direct drive fan engines and 1.3, 1.4, 1.5, and 1.6 for the geared fan engines. For the direct drive engines both "high work" and "low work" LPC approaches were examined. Since the benefits of the geared fan design are most pronounced when the low-spool is required to do a large amount of compression work, the low work, geared fan combination was not modeled. As found in the previous work, a variable area fan nozzle was only needed for fan pressure ratios of 1.4 and below. Not all combinations of parameters necessarily lead to practical designs. An exceptionally large engine diameter is an issue for the geared, FPR=1.3 engine. The large diameter leads to a long landing gear given the under-wing engine integration approach assumed for the study. More detailed analysis would be necessary to determine if such a long landing gear could be practically accommodated. The direct drive, FPR=1.4 design is an extreme case for the direct drive engine architecture. Under the design ground rules used for this study, the slow low-spool speed of this engine necessitates a large number of LPT stages, leading to an extremely heavy and long engine. These "impractical" engines were carried forward through the remainder of the analyses, however, in order to investigate performance trends as FPR is decreased to the extreme. There may also be practicality issues for the FPR=1.6 geared engine. Although the fan gear ratio for the FPR=1.3 engine is 3.6, this ratio decreases to only 1.6 for the FPR=1.6 geared engine. Gear ratios close to 1.0 may be difficult to justify from a mechanical design standpoint since any weight or performance benefits that might result would likely be overwhelmed by the increased design and operational costs associated with the gearbox.

Table 2. Engine Trade Space

Engine Designation	Fan Drive	Fan Nozzle	ADP	FPR	OPR	LPC PR	HPC PR
Lo-dd-1.4*	Direct	Variable	M0.80/35kft	1.4	42	1.69	17.7
Lo-dd-1.5	Direct	Fixed	M0.80/35kft	1.5	42	1.58	17.7
Lo-dd-1.6	Direct	Fixed	M0.80/35kft	1.6	42	1.48	17.7
Lo-dd-1.7	Direct	Fixed	M0.80/35kft	1.7	42	1.39	17.7
Hi-dd-1.4*	Direct	Variable	M0.80/35kft	1.4	42	2.50	12.0
Hi-dd-1.5	Direct	Fixed	M0.80/35kft	1.5	42	2.33	12.0
Hi-dd-1.6	Direct	Fixed	M0.80/35kft	1.6	42	2.19	12.0
Hi-dd-1.7	Direct	Fixed	M0.80/35kft	1.7	42	2.06	12.0
Hi-g-1.3*	Geared	Variable	M0.80/35kft	1.3	42	2.69	12.0
Hi-g-1.4	Geared	Variable	M0.80/35kft	1.4	42	2.50	12.0
Hi-g-1.5	Geared	Fixed	M0.80/35kft	1.5	42	2.33	12.0
Hi-g-1.6	Geared	Fixed	M0.80/35kft	1.6	42	2.19	12.0

*Design ground rules lead to practicality issues for these cases.

General characteristics of the low work and high work engine designs are shown in Tables 3 and 4, respectively. The counter trends of increasing engine size and weight versus decreasing TSFC as FPR is decreased are clearly evident in both the low work and high work designs. For the low work engines, TSFC at ADP decreases from 0.525 lb/(lb-h) with a FPR of 1.7 to 0.479 lb/(lb-h) with a FPR of 1.4 (-9%), reflecting the improvement in propulsive efficiency associated with increasing BPR from 10 to 19. Note that even at a FPR=1.7, high by today's standards, the BPR of 10 is much higher than that of current engines in this thrust class. The higher BPR for a given FPR compared to current engines is a reflection of the significant reduction in core size enabled by the advanced technologies assumed in the engine design.

The TSFC improvement with lower FPR comes with a significant increase in engine weight. The weight of the direct drive, FPR=1.4 engine is 73% more than the direct drive, FPR=1.7 design. The geared fan approach included in the high work designs does mitigate the weight penalty associated with low FPR. The geared, high work FPR=1.4 engine is only 15% heavier than the direct drive, high work FPR=1.7 engine, while retaining a 8% TSFC benefit. Even though the geared fan approach decreases the weight penalties of low FPR, the issues associated with increased nacelle drag and engine integration remain.

Table 3. General Characteristics of Low Work Engines

	Lo-dd-1.4*		Lo-dd-1.5		Lo-dd-1.6		Lo-dd-1.7	
Fan Drive/Gear Ratio	Direct Drive		Direct Drive		Direct Drive		Direct Drive	
Fan Diameter, in	81		74		69		66	
Fan Nozzle Geometry	Variable		Fixed		Fixed		Fixed	
Engine+Nacelle Weight, lb	10563		7965		6592		6099	
Nacelle Max Diameter, ft	8.3		7.6		7.1		6.7	
Operating Conditions	SLS	TOC	SLS	TOC	SLS	TOC	SLS	TOC
Fan Pressure Ratio	1.3	1.4	1.4	1.5	1.5	1.6	1.6	1.7
Bypass Ratio	18.4	18.8	15.0	14.8	12.7	12.5	10.9	10.5
Overall Pressure Ratio	33.1	42	33.8	42	34.4	42	35	42
Net Thrust, lb	23813	5000	23370	5000	23046	5000	22734	5000
TSFC, lb/(lb-h)	0.233	0.479	0.253	0.495	0.271	0.510	0.290	0.525
NO_X Emission Index (g/kg)	25.4	8.1	25.8	7.8	26.4	7.6	26.9	7.4

*Design ground rules lead to practicality issues for this case.

Table 4. General Characteristics of High Work Engines

	Hi-g-1.3*		Hi-g-1.4		Hi-dd-1.4*		Hi-g-1.5		Hi-dd-1.5		Hi-g-1.6		Hi-dd-1.6		Hi-dd-1.7	
Fan Drive/Gear Ratio	Geared/3.6		Geared/2.6		Direct Drive		Geared/2.0		Direct Drive		Geared/1.6		Direct Drive		Direct Drive	
Fan Diameter, in	90		80		80		74		74		69		69		66	
Fan Nozzle Geometry	Variable		Variable		Variable		Fixed		Fixed		Fixed		Fixed		Fixed	
Engine+Nacelle Weight, lb	8736		7401		11292		6626		8821		6252		7276		6451	
Nacelle Max Diameter, ft	9.3		8.2		8.2		7.6		7.6		7.1		7.1		6.7	
Operating Conditions	SLS	TOC	SLS	TOC	SLS	TOC	SLS	TOC	SLS	TOC	SLS	TOC	SLS	TOC	SLS	TOC
Fan Pressure Ratio	1.2	1.3	1.3	1.4	1.3	1.4	1.4	1.5	1.4	1.5	1.5	1.6	1.5	1.6	1.6	1.7
Bypass Ratio	24.3	24.2	17.6	17.5	17.8	17.7	14.7	14.3	14.8	14.4	12.4	11.8	12.6	12.0	10.8	10.2
Overall Pressure Ratio	31.7	42	32.9	42	32.9	42	32.7	42	32.7	42	33.1	42	33.1	42	33.6	42
Net Thrust, lb	26343	5000	24917	5000	24915	5000	23369	5000	23365	5000	22924	5000	22920	5000	22561	5000
TSFC, lb/(lb-h)	0.204	0.470	0.236	0.486	0.234	0.481	0.257	0.502	0.254	0.497	0.276	0.517	0.273	0.512	0.292	0.527
NO_X Emission Index (g/kg)	23.9	7.8	24.9	7.1	24.9	7.1	24.6	7.3	24.6	7.3	25.0	7.0	24.9	7.0	25.4	6.8

*Design ground rules lead to practicality issues for these cases.

4.2 Engine Comparison

Variation of engine characteristics with FPR and comparisons to the equivalent “Spiral 2” engines of the previous study are shown graphically in Figures 2 through 6. The “Spiral 2” results of the previous study are shown as faded lines in the figures and the lowest FPR points are connected with dashed lines to indicate the practicality issues with those designs. The relationship between BPR and FPR is shown in Figure 2. As FPR is decreased to 1.3, BPR increases to nearly 25, almost 5 times that of the CFM56-7B engines currently used on the Boeing 737. Bypass ratios for the new engines are generally slightly higher than for the engines of the previous study. The increase in BPR is primarily associated with a reduction in total chargeable cooling resulting from the change in LPT cooling philosophy. As the demand for cooling air decreases, the core size decreases, increasing the BPR. The removal of the uncooled LPT constraint greatly reduced the HPT chargeable cooling for the high work designs. In the low work engines, more of the thermal energy entering the HPT is converted to work to power the HPC (which has a higher pressure ratio compared to the equivalent high work engine) and less HPT chargeable cooling was required to achieve an uncooled LPT. The change in cooling philosophy therefore had a much smaller impact on the low work designs. At a FPR of 1.5, the BPR increased 10% for the high work engines and only 3.5% for the low work engine.

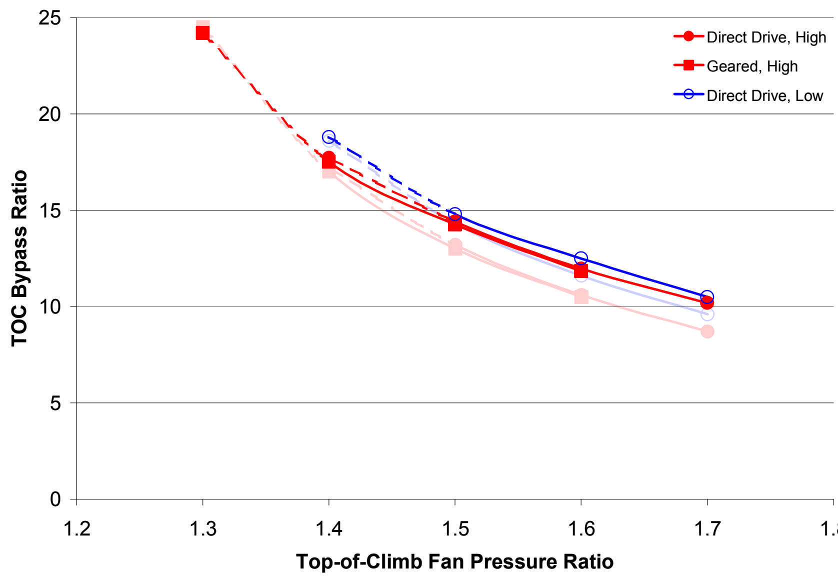

Figure 2. Relationship between bypass ratio and design fan pressure ratio, TOC conditions.

The variation of TSFC with FPR is approximately linear as shown in Figure 3. The efficiency benefits of lower FPR are clearly evident with an ~11% decrease in TSFC as FPR is decreased from 1.7 to 1.3. At a given FPR, the geared fan engine has slightly higher TSFC than the equivalent direct drive engine due mainly to gearbox losses, but the difference is only ~1%. The changes in engine modeling assumptions for the current study had little impact on the TSFC characteristics of the low work engines, but resulted in a downward shift of the TSFC curves for the high work engines. The change in LPT cooling philosophy and associated cycle changes as discussed above are primarily responsible for this reduction in TSFC for the high work engines. The TSFC penalty of the high work approach seen in the previous study is essentially eliminated with the new engines.

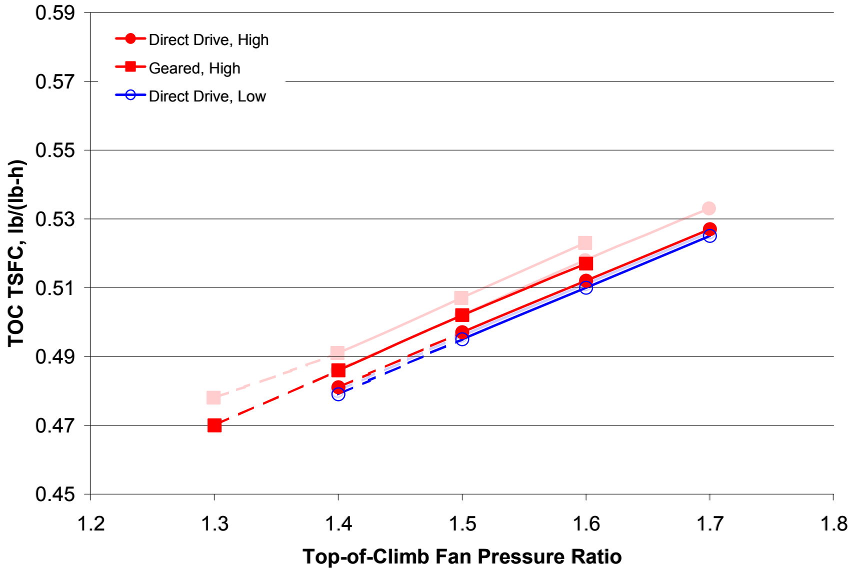

Figure 3. Variation of TSFC with engine type and design fan pressure ratio, TOC conditions.

The variation of engine size (nacelle diameter) with FPR is shown in Figure 4. The choice of high work versus low work, or direct drive versus geared fan has no impact on the engine size. In all cases, as FPR is decreased, the fan diameter (and therefore nacelle diameter) must increase to provide the required design thrust. There is also essentially no size difference between the engines in this study and the "Spiral 2" engines in reference 2.

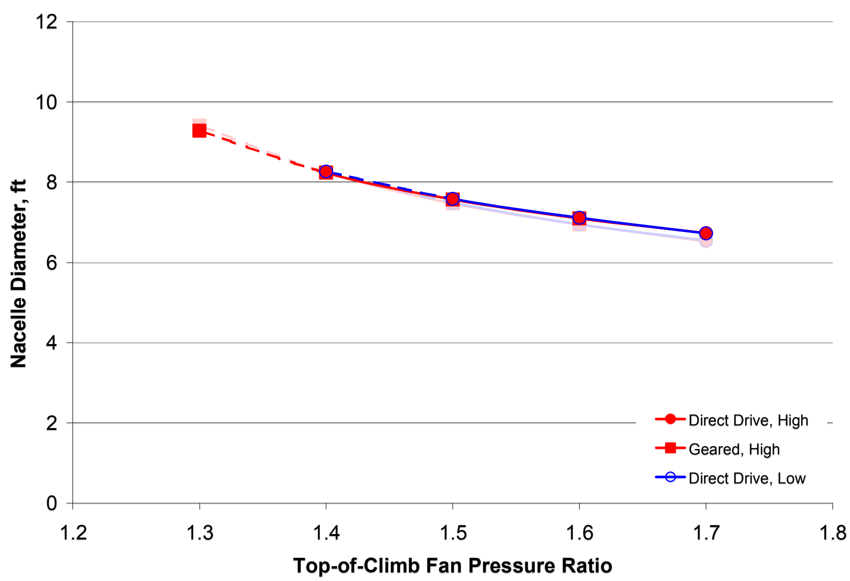

Figure 4. Variation of nacelle maximum diameter with engine type and design fan pressure ratio.

Engine weight estimates are presented in Figure 5. For both the direct drive and geared fan engines, there is a sizable weight penalty associated with decreasing FPR; however, this penalty is much less severe for the geared fan architecture. As FPR is reduced, the fan and overall diameter of the engine become larger, leading to higher fan and nacelle weight. This is the primary cause of the increased weight of the low FPR geared engines. For the direct drive engines, as the FPR and fan rotational speed decrease, so does the rotational speed of the directly connected LPT. At a slower speed, more LPT stages are needed resulting in an additional weight penalty not present in the geared designs. For the geared engines, LPT rotational speed can remain high as FPR is reduced and LPT weight varies little with FPR. The new design assumptions had little impact on the weight trends, but did result in an approximately 6% increase in engine weight for the direct drive engines. In general this weight increase is due to higher component diameters and/or additional stages. For example, an additional LPT stage was required for most of the high work, direct drive designs to meet the higher LPT work output of the revised engine cycles while keeping LPT loading the same. The geared engines can more readily accommodate these types of changes with minimal weight impact through changes in the gear ratio. For example, only a slight (<5%) increase in the gear ratio was necessary to accommodate the increase in LPT work, with no changes in the LPT loading or number of stages.

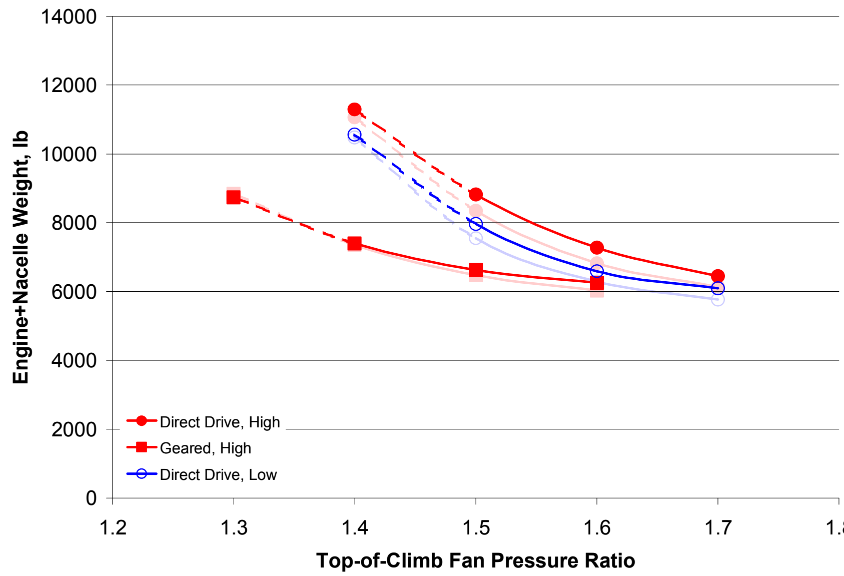

Figure 5. Variation of engine+nacelle weight with engine type and design fan pressure ratio.

The comparison in Figure 5 is not completely valid because of the difference in the thrust sizing points for the current and previously designed engines. Although all the engines represented in Figure 5 have equal thrust at Mach 0.8, 35,000ft, the sea level static and rolling takeoff thrusts vary. In Figure 6, the weight data is presented in terms of engine thrust-to-weight ratio (T/W) at the rolling takeoff condition (M=0.25, SL). Although the thrust-to-weight ratios for the current engines are lower at high FPR, the T/W curves are flatter than for the engines of reference 2. In other words, with the new design approach of using rolling takeoff as a thrust sizing point, the weight penalty to provide equal thrust at rolling takeoff as FPR is lowered has been reduced. This results in higher takeoff T/W at low FPR. Since takeoff performance was an active constraint in the aircraft sizing analysis of reference 2, this should result in better overall aircraft system level performance for the low FPR engines.

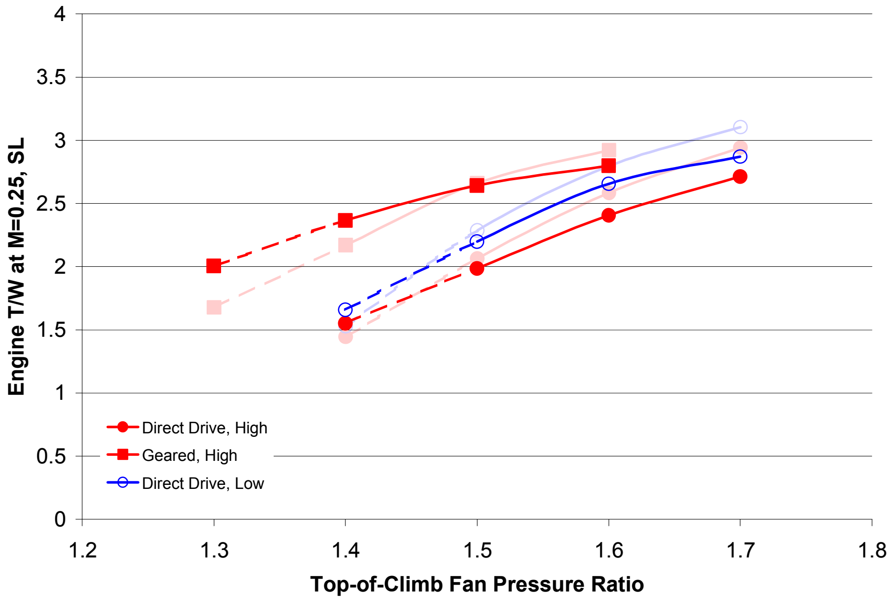

Figure 6. Variation of engine thrust-to-weight ratio with engine type and design fan pressure ratio.

5.0 Aircraft Sizing and Performance Results

It is not clear from the engine characteristics alone what impact the revised engine designs will have on the conclusions of reference 2. For the low work, direct drive engines, TSFC is approximately the same, but weight is higher. For the high work engines there is a decrease in TSFC, but an increase in weight, although only a very slight increase for the geared fan engines. Only by combining the engines with the airframe model can the net impact of these changes on metrics such as block fuel consumption be determined. For each of the engine cases, FLOPS (with additional external analyses for wing weight, fuselage weight, landing gear size, vertical tail size, and engine-out drag) was used to size/optimize the gross weight, wing area, and thrust needed to perform the design mission. Other design parameters such as wing aspect ratio and wing taper ratio were held fixed at the 737-800 values. Constraints used in wing and engine sizing included: wing fuel capacity, approach speed, missed approach climb, second segment climb, takeoff field length, and initial cruise altitude capability (expressed as minimum potential rate-of-climb of 300 ft/min at M=0.8, 35,000ft). Other performance aspects of the configurations (e.g., landing field length) were also checked for reasonableness following completion of the sizing/optimization.

Results of the aircraft sizing analysis are summarized in Table 5 for the low work engines and Table 6 for the high work engines. The numbers in bold indicate the “best” value for that particular parameter. Results for a 1998 entry-into-service (EIS) technology baseline vehicle (similar to a 737-800 with CFM56-7B engines, but sized to perform the study design mission) are shown in the tables for comparison. For the low work, direct drive engines, block fuel consumption is minimized with a design FPR of 1.6. The BPR for this engine is 12.5 at ADP conditions. Note that the cruise range factor, which is an approximate measure of combined aerodynamic and propulsive efficiency, increases at lower FPR. However, this higher efficiency is insufficient to offset the increase in weight that occurs for the lower FPR engines. This clearly illustrates the system level trade-off that occurs for lower FPR engines, the benefit of higher efficiency versus the penalty of higher weight. Although the minimum fuel consumption case is at FPR=1.6, the minimum gross weight occurs at FPR=1.7. In other words, the decrease in engine weight for that configuration is sufficient to offset the increase in fuel weight to arrive at a lower total gross weight. Lowest total NO_X emissions (referred to as “block NO_X” in the table) also occur with a FPR=1.7 design. Landing-takeoff cycle (LTO) NO_X emissions are lowest for the FPR=1.4 engine; but, the variation in LTO NO_X is relatively small among all the cases. Clearly, identifying a “best” engine design depends on the metric of interest. Ultimately the primary metric is life cycle cost, and historically gross weight has been used as a surrogate for life cycle cost in aircraft design and optimization. However, recent increases in fuel cost have made fuel consumption a more important factor in life cycle cost. It may no longer be valid to assume the lowest gross weight configuration has the lowest life cycle cost.

Sizing results for the high work engine cases are given in Table 6. Both geared and direct drive fan approaches were considered for the high work engines. The lowest block fuel consumption occurs for the geared, FPR=1.5 engine case. The BPR of this engine is 14.3 at ADP conditions. As with the low work engines, there is a trade-off between the efficiency associated with lower FPR and the increase in engine weight. The FPR=1.3 and FPR=1.4 geared fan cases have higher cruise efficiency, but also higher block fuel consumption. The geared, FPR=1.6 case provides the lowest total NO_X emissions and lowest ramp weight. The lowest LTO NO_X emissions occur at the opposite end of the fan pressure ratio spectrum, at FPR=1.3. The geared fan system is able to mitigate to some extent the penalties associated with decreasing FPR and increasing BPR. This benefit can be seen by comparing the FPR=1.4 results in Table 6 for the two different fan drive approaches. The aircraft with the geared fan engine has a lower empty weight, lower ramp weight, lower block fuel consumption, lower total NO_X and lower LTO NO_X emissions. But, even in the case of geared designs, minimum block fuel occurs at a FPR of 1.5, not at lower FPR where cruise efficiency is higher.

Most of the aircraft in Tables 5 and 6, have lower wing loading than is typical for a 737-800 like design. For the chosen design mission and constraints, takeoff field length is the primary sizing constraint, which can be met by a range of different engine and wing sizes. The penalty of increasing wing size is diminished somewhat for the ASAT configurations relative to current designs due to the use of composite materials. As a result, for the ASAT designs the preferred (lower gross weight) approach to meeting the takeoff requirement tends to be a larger wing (low wing loading) rather than a larger engine (high thrust-to-weight). This lower wing loading also reduces approach speed, benefiting approach noise levels.

Table 5. Aircraft Sizing Results for Low Work Engines (162 Passenger, 3250 nm Design Mission)

	1998 Tech. Baseline	**Lo-dd-1.4* (BPR ~ 19)**	**Lo-dd-1.5 (BPR ~ 15)**	**Lo-dd-1.6 (BPR ~ 13)**	**Lo-dd-1.7 (BPR ~ 11)**
OEW, lb	*94700*	97450	87300	82800	**81400**
Mission Fuel, lb	*50350*	38750	36700	**36400**	37000
Payload Weight, lb	*32400*	32400	32400	32400	32400
Ramp Weight, lb	*177550*	168600	156400	151600	**150800**
Wing Area, ft^2	*1470*	1450	1390	1330	1320
W/S, lb/ft^2	*121*	116	112	114	114
Thrust(SLS), lb	*26100*	26100	23600	22900	22650
T/W (takeoff)	*0.294*	0.310	0.302	0.303	0.300
Takeoff field length, ft	*7000*	7000	7000	7000	7000
Landing field length, ft	*6020*	5850	5700	5740	5750
~Cruise Range Factor V*(L/D)/TSFC, nm	*12450*	**15600**	15300	15000	14700
Block Fuel, lb	*42600*	32900	31100	**30800**	31250
Block NO_X, lb	*555*	245	226	218	**216**
LTO NO_X, lb per cycle	*22.2*	**10.7**	11.0	11.1	11.8

*Design ground rules lead to practicality issues for this case.

Table 6. Aircraft Sizing Results for High Work Engines (162 Passenger, 3250 nm Design Mission)

	1998 Tech. Baseline	**Hi-g-1.3* (BPR ~ 24)**	**Hi-g-1.4 (BPR ~ 18)**	**Hi-dd-1.4* (BPR ~ 18)**	**Hi-g-1.5 (BPR ~ 15)**	**Hi-dd-1.5 (BPR ~ 15)**	**Hi-g-1.6 (BPR ~ 12)**	**Hi-dd-1.6 (BPR ~ 12)**	**Hi-dd-1.7 (BPR ~ 11)**
OEW, lb	*94700*	90200	85300	101050	83000	90650	**81950**	85150	82750
Mission Fuel, lb	*50350*	36400	36100	40800	**35850**	38000	36600	37300	37550
Payload Weight, lb	*32400*	32400	32400	32400	32400	32400	32400	32400	32400
Ramp Weight, lb	*177550*	158950	153800	174200	151200	161000	**151000**	154800	152700
Wing Area, ft^2	*1470*	1340	1340	1460	1340	1420	1325	1380	1350
W/S, lb/ft^2	*121*	119	114	120	113	114	114	112	113
Thrust(SLS), lb	*26100*	27650	24800	28350	23200	24400	22900	23100	22600
T/W (takeoff)	*0.294*	0.348	0.323	0.325	0.306	0.303	0.303	0.298	0.296
Takeoff field length, ft	*7000*	7000	7000	7000	7000	7000	7000	7000	7000
Landing field length, ft	*6020*	5940	5780	5970	5730	5750	5760	5700	5720
~Cruise Range Factor V*(L/D)/TSFC, nm	*12450*	**15600**	15300	15300	15100	15200	14800	14900	14600
Block Fuel, lb	*42600*	30900	30600	34550	**30400**	32200	31000	31600	31800
Block NO_X, lb	*555*	226	215	242	210	224	**209**	215	210
LTO NO_X, lb per cycle	*22.2*	**9.3**	10.0	11.3	10.0	10.4	10.6	10.6	11.2

*Design ground rules lead to practicality issues for these cases.

The weight, fuel consumption, and NO_X results are presented graphically in Figures 7 through 13, overlaid on the reference 2 results. Aircraft empty weight results are compared in Figure 7. Consistent with the trends in engine weight, aircraft empty weight increases as FPR is decreased. Also, the increase in engine weight relative to reference 2 is reflected in the generally higher aircraft empty weights for the current analysis. Trends are similar to the previous results, although the curves are flatter and empty weight is now less sensitive to FPR than before. This is particularly true for the high work, geared engine cases in which the previous empty weight penalty of ~20,000 lb associated with decreasing FPR from 1.6 to 1.3 has been reduced to only 8,250 lb.

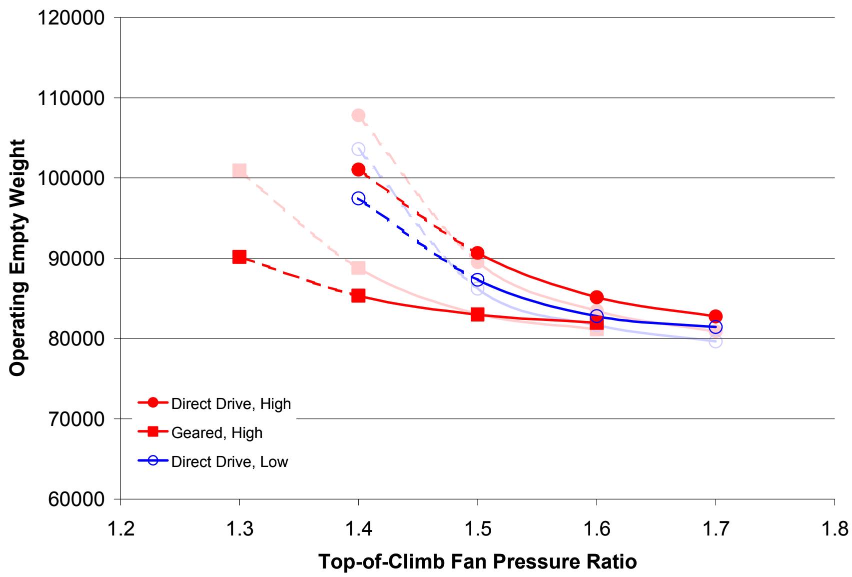

Figure 7. Variation of aircraft empty weight with engine type and design fan pressure ratio.

The impacts of the engine design changes on ramp weight are similar to the impacts on empty weight. The results presented in Figure 8 indicate higher ramp weights for FPRs of 1.6 and 1.7, similar ramp weights for FPR=1.5, and lower ramp weights for the low FPRs of 1.3 and 1.4. Although the sensitivity of ramp weight to FPR has been reduced, the lowest ramp weight cases still occur for the highest fan pressure ratios analyzed.

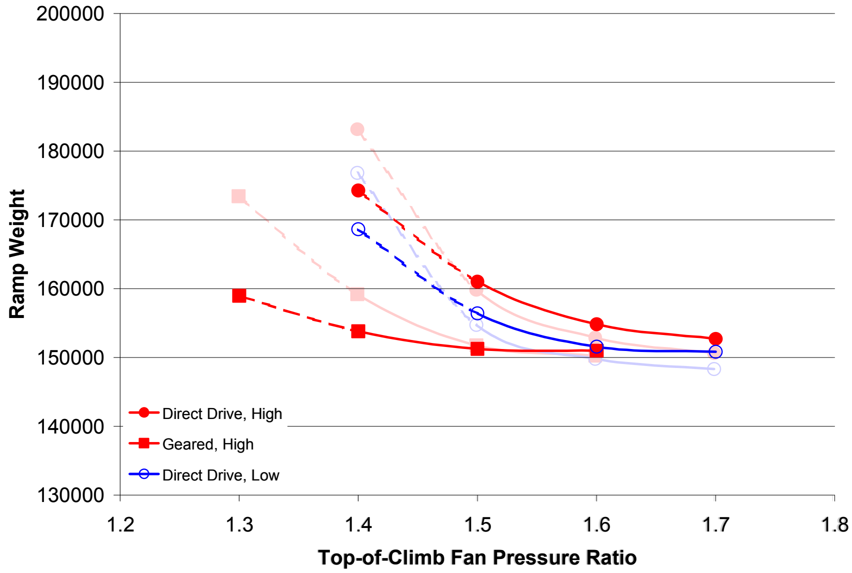

Figure 8. Variation of aircraft ramp weight with engine type and design fan pressure ratio.

Fuel consumption results are presented in Figure 9. For the direct drive engines, the same trends are observed as in the results of reference 2. For both low work and high work cases, minimum block fuel consumption occurs with a FPR of 1.6. The new engines result in slightly higher fuel consumption for FPR of 1.5 to 1.7 and lower fuel consumption for FPR of 1.4. The engine design changes had greater impacts on the high work geared engine cases. The high work geared cases benefited from both a decrease in TSFC (Figure 3) and an increase in thrust-to-weight at the rolling takeoff condition (Figure 6). Fuel consumption is reduced in all cases, and reducing FPR has a much smaller negative affect on the fuel consumption due to lower engine weight penalties for low FPR (flatter curve in Figure 6). Note, however, that although the variation of fuel consumption with FPR is fairly small for the geared, high work engines, the minimum block fuel still occurs at a FPR of 1.5, as was also found in reference 2. The engine design changes have not changed the optimum FPR for fuel consumption for a given engine architecture, but the overall minimum fuel case has changed. Previously the overall minimum fuel consumption occurred for the low work, direct drive fan, FPR=1.6 case. With the changes in engine design, the minimum fuel consumption now occurs for the high work, geared fan, FPR=1.5 case. The “cross over” FPR below which the geared fan approach results in lower fuel consumption than the low work, direct drive approach has also moved from FPR=1.5 to FRP~1.55. Although the geared fan, FPR=1.5 case results in the lowest fuel consumption of all the cases, the low work, direct drive FPR=1.6 case has a fuel consumption that is only 1.3% higher. Given the high level nature of this analysis, these two cases can be considered essentially equivalent from a fuel consumption perspective. The lower fan pressure ratio of the geared fan, FPR=1.5 case leads to lower noise, however, as will be discussed later.

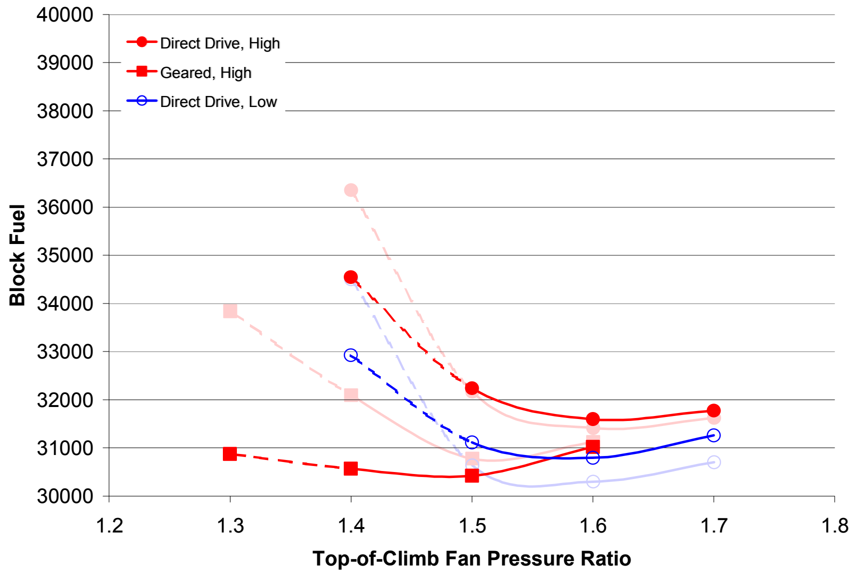

Figure 9. Variation of block fuel with engine type and design fan pressure ratio.

For total NO_X, shown in Figure 10, the minimum NO_X emissions occur at the highest FPR analyzed for all the engine architectures. Results are similar between the high work and low work direct drive cases, while the high work geared fan engines result in lower total NO_X emissions, particularly at low FPRs. Compared to the results of reference 2, the NO_X is higher for high FPR cases and lower for low FPR cases, reflecting the same "flattening" of the curves as seen in the other metrics.

The landing-takeoff cycle NO_X (LTO NO_X) can be expressed in a number of different ways. LTO NO_X is regulated as an engine parameter, "D_p/F_{oo}" where D_p is the grams of NO_X emitted over a standard LTO cycle (by a single, uninstalled engine) and F_{oo} is the rated output at SLS conditions in kilonewtons. This parameter is defined by the International Civil Aviation Organization (ICAO) and used in FAR Part 34 for engine certification (ref. 22). The results for D_p/F_{oo} are presented in Figure 11; results are similar to those obtained in reference 2. There is a consistent downward trend in D_p/F_{oo} with decreasing fan pressure ratio. Another way to view LTO NO_X is the margin relative to the current CAEP6 regulatory limit, as shown in Figure 12. CAEP6 refers to the limits adopted at the sixth meeting of the ICAO Council Committee on Aviation Environmental Protection (CAEP), held in 2004. Not only does lower FPR decrease D_p/F_{oo}, it also increases the margin relative to the regulation. Note that all of the engines are predicted to meet or exceed NASA's CAEP6-60% goal for the "N+1" timeframe. The D_p/F_{oo} emission parameter alone does not account for differences in engine weight and performance which can lead to differences in the required thrust level (F_{oo}) when the engine is integrated into an overall aircraft design. Lower D_p/F_{oo} does not necessarily result in lower total LTO NO_X emissions. The estimated NO_X per LTO cycle is compared in Figure 13. NO_X per LTO cycle has been estimated by multiplying the ICAO D_p/F_{oo} parameter by the total engine thrust. The trends shown in Figure 13, are not as consistent as the other metrics. High FPR certainly leads to higher NO_X, but between FPR=1.3 and 1.5 the variation with FPR is not consistent. The NO_X per LTO cycle results depend on a combination of the engine characteristics (D_p/F_{oo}) and the aircraft sizing results (e.g., trade between engine thrust and wing area necessary to meet takeoff performance); therefore, they exhibit more variability.

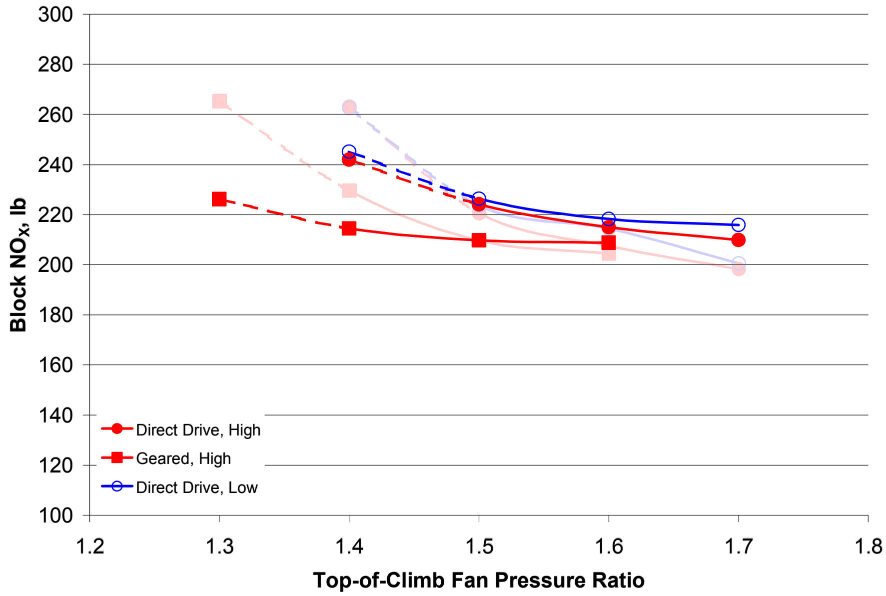

Figure 10. Variation of total mission NO_X emissions with engine type and design fan pressure ratio.

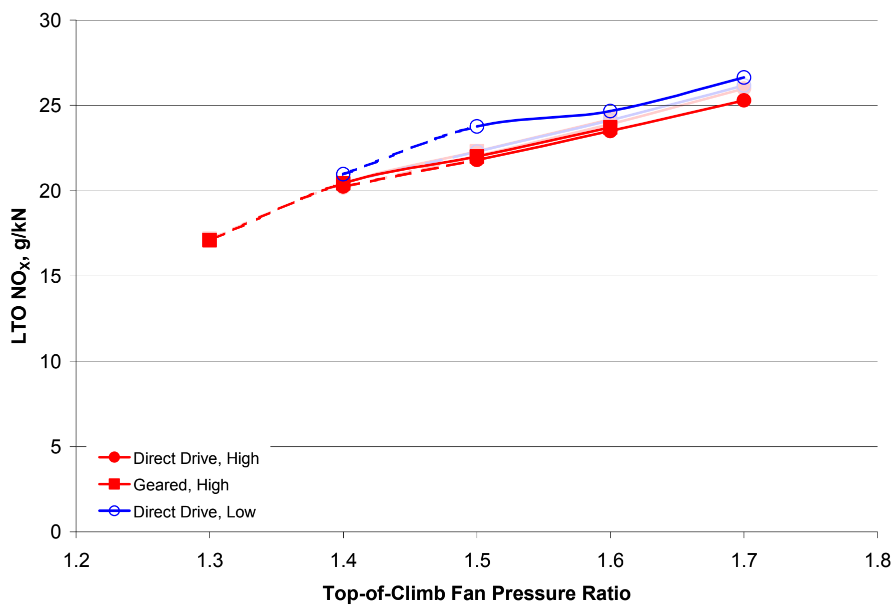

Figure 11. Variation of LTO NO_X emissions with engine type and design fan pressure ratio (D_p/F_{oo}).

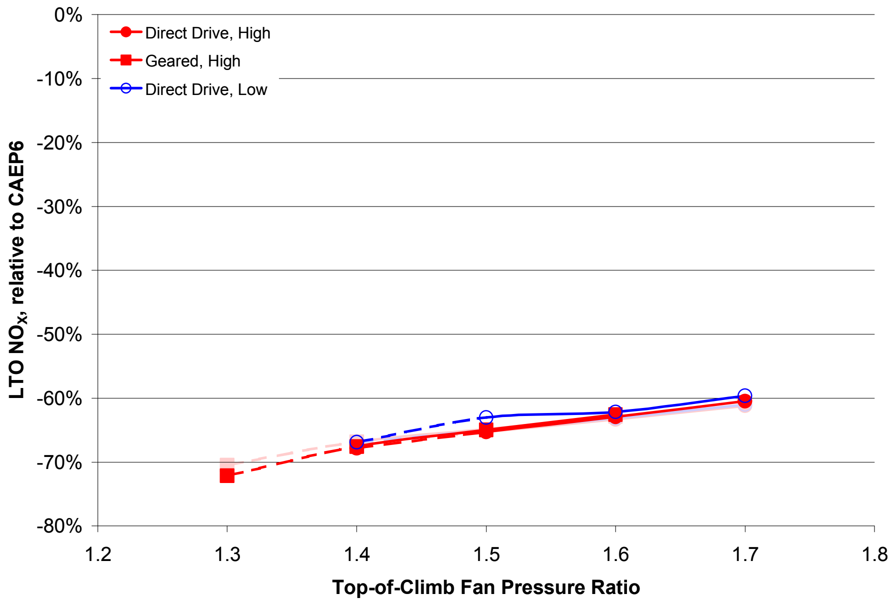

Figure 12. LTO NO_X margin relative to CAEP6 regulatory limit.

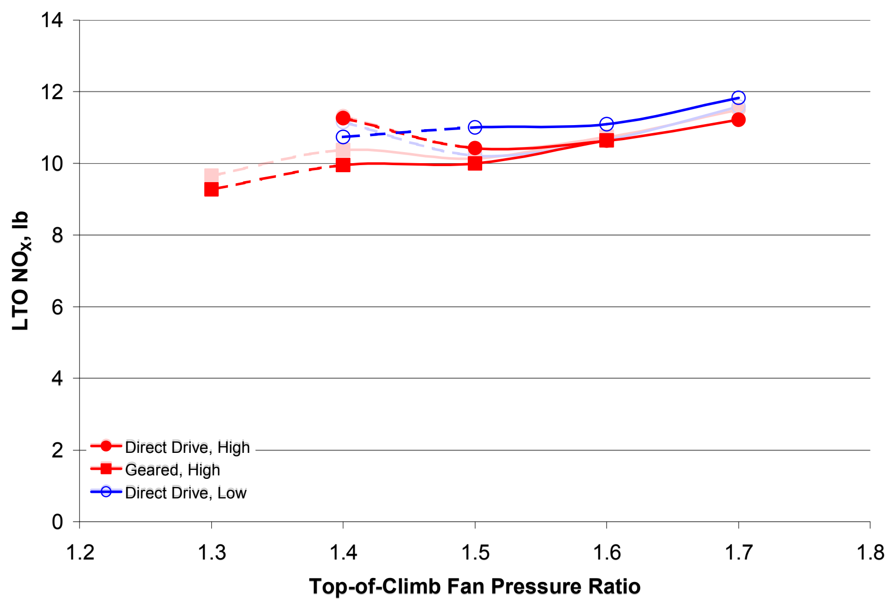

Figure 13. Variation of NO_X emissions per LTO cycle with engine type and design fan pressure ratio.

Overall fuel, weight, and NO_X benefits of the ASAT engine and airframe technologies are shown in Figures 14 through 17. Regardless of the engine design chosen, fuel burn reduction relative to the 1998 technology baseline is in the range of 25-30% (Figure 14), with the largest reduction of 28.6% for the high work, geared, FPR=1.5 engine design. These significant reductions in block fuel are a result of the combination of advanced airframe and engine technology assumptions, in addition to the engine cycle changes. Reductions in ramp weight on the order of 15% are possible as well, as shown in Figure 15. The advanced combustor technology assumed for the engines in this study results in large reductions in both total NO_X and LTO NO_X. Reductions of 60% in total NO_X and 50-60% in LTO NO_X are estimated for the advanced ASAT vehicles as shown in Figure 16 and Figure 17, respectively.

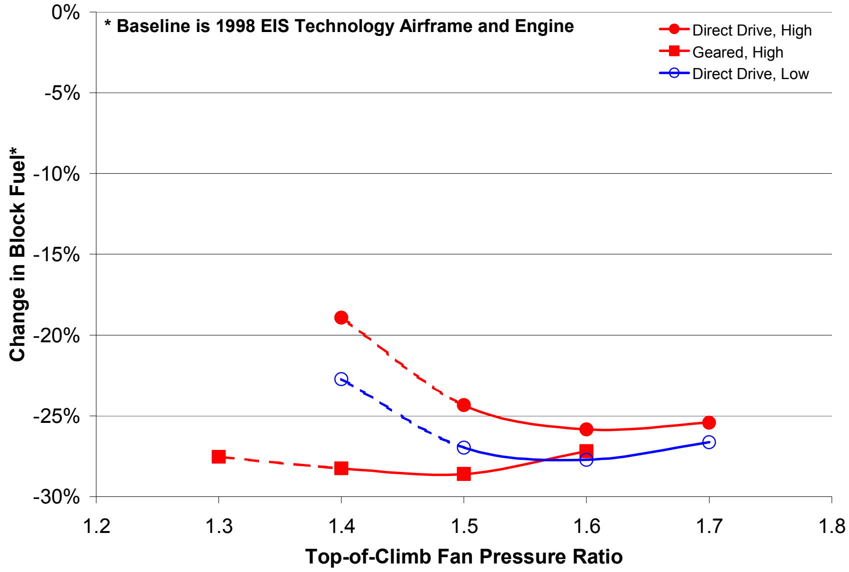

Figure 14. Potential block fuel reductions from application of ASAT technologies.

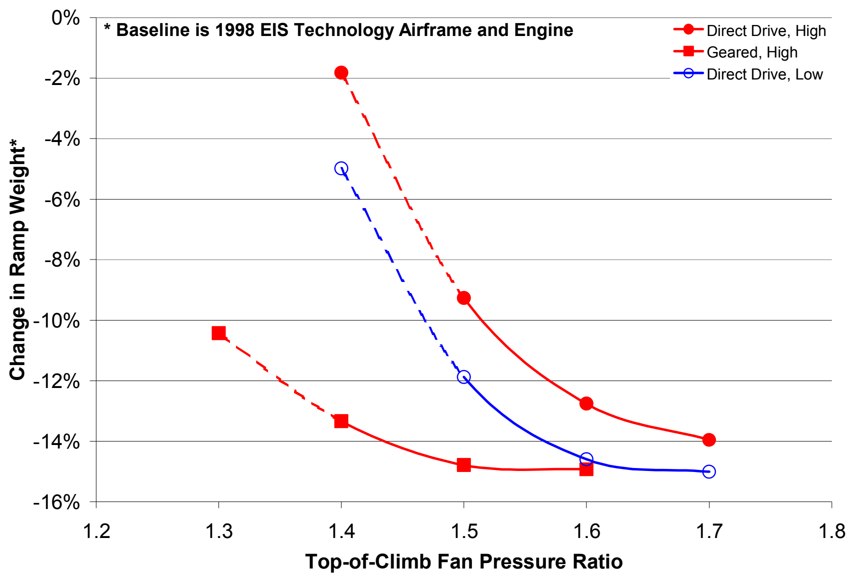

Figure 15. Potential ramp weight reductions from application of ASAT technologies.

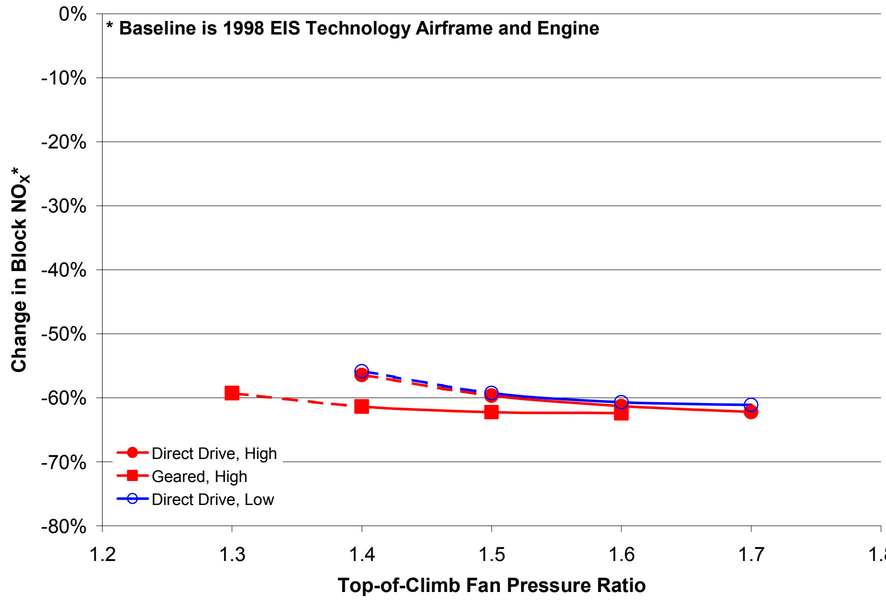

Figure 16. Potential total NO_X reductions from application of ASAT technologies.

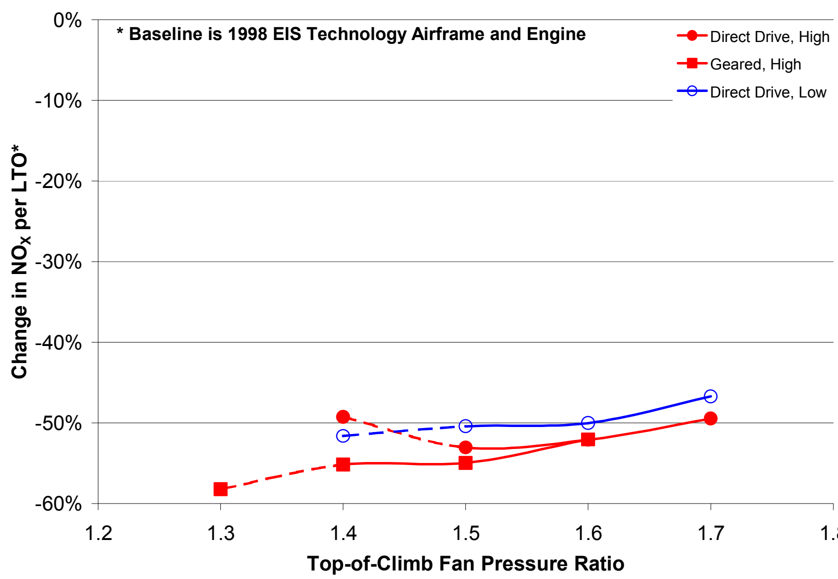

Figure 17. Potential LTO NO_X reductions from application of ASAT technologies.

Noise benefits for the ASAT configurations are shown in Figure 18. Often certification noise is expressed in terms of the algebraic sum of the lateral, flyover, and approach noise levels ("cumulative noise"). The cumulative noise reductions for the study configurations relative to the 737-800 predicted value are presented in Figure 18. The noise reduction estimates from reference 2 are also shown for comparison. As found previously in reference 2, the noise results are dominated by FPR. Fan drive approach and compression work split have little impact on the noise characteristics. The positive impact of low FPR on noise is clearly evident. The cumulative noise reduction achieved by reducing FPR from 1.7 to 1.3 is over 21 EPNdB; despite the higher aircraft weight and engine thrust associated with FPR=1.3

case. The maximum reduction relative to the 737-800 baseline realized for a practical design is 25.3 EPNdB cumulative (geared, FPR=1.4 case). This reduction is the result of both engine cycle changes and noise reduction technologies. At FPR=1.3, the cumulative noise reduction is over 30 EPNdB. The FPR=1.3 case in this study results in an aircraft design with landing gear length issues. However, there may be other integration approaches which would enable the additional noise benefit of the FPR=1.3 engine to be realized in a practical aircraft design. It was previously noted that the fuel consumption characteristics of the minimum fuel case (low work, geared fan, FPR=1.5) could be nearly achieved with the low work, direct drive fan, FPR=1.6 case. The geared, FPR=1.5 approach, however, results in 6.7 EPNdB lower cumulative noise than the direct drive, FRP=1.6 case, as can be observed in Figure 18. Although the geared engines do not offer a significant fuel consumption benefit over the direct drive engines, they do offer the potential for significantly lower noise with equivalent fuel consumption. Compared to the results in reference 2, the changes in engine design have generally resulted in a slight decrease in cumulative noise of approximately 2 EPNdB or less.

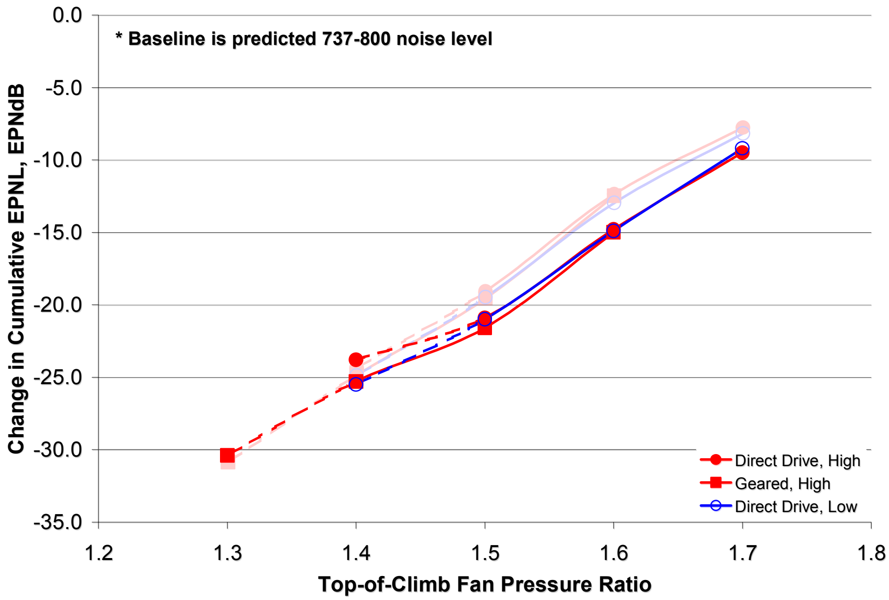

Figure 18. Potential noise reductions from application of ASAT technologies.

6.0 Design Trade-Offs

Since no single engine provides the best performance across all of the metrics, there are a series of design trade-offs that must be accepted. For example, choosing a very low FPR because of the noise benefits incurs an increase in aircraft weight compared to what could be achieved with a higher FPR design. The magnitudes of these various trade-offs are presented in Table 7. Similar analysis was also performed in reference 2 and those results are shown in parentheses in Table 7. For each metric column, the minimum value is used as the baseline for the remaining cases. The values in the remaining rows indicate the magnitude of the penalty incurred from selecting that particular engine, relative to the best possible result. For example, the direct drive, low work, FPR=1.5 case has 3.7% higher ramp weight than the minimum (direct drive, low work LPC, FPR=1.7); 2.3% greater block fuel consumption than the minimum (geared, high work LPC, FPR=1.5); 8.4% greater block NO_X than the minimum (geared, high work LPC, FPR=1.6); 10.6% greater LTO NO_X than the minimum (geared, high work LPC, FPR=1.4); and 4.3 EPNdB higher cumulative noise than the minimum (geared, high work LPC, FPR=1.4). (The geared, FPR=1.3 and direct drive, FPR=1.4 cases were not included in the trade-off analysis because of the practicality issues with those designs.)

Table 7. Weight, Fuel, Emissions, and Noise Trade-Offs

	Ramp Weight	Block Fuel	Block NO_X	LTO NO_X	Cum. EPNdB
High, Geared, FPR=1.4	**+2.0 %** (+7.3%)	**+0.5%** (+5.9%)	**+2.7%** (+15.8%)	**Minimum** (+2.3%)	**Minimum** (Minimum)
High, Geared, FPR=1.5	**+0.3%** (+2.3%)	**Minimum** (+1.6%)	**+0.5%** (+5.8%)	**+0.5%** (Minimum)	**+3.7** (+5.3)
Low, Direct, FPR=1.5	+3.7% (+4.3%)	+2.3% (+1.1%)	+8.4% (+12.8%)	+10.6% (+0.8%)	+4.3 (+5.4)
High, Direct, FPR=1.5	+6.8% (+7.8%)	+6.0% (+6.2%)	+7.3% (+11.2%)	+4.8% (+2.8%)	+4.4 (+5.8)
High, Geared, FPR=1.6	**+0.1%** (+1.3%)	**+2.0%** (+2.7%)	**Minimum** (+3.1%)	**+6.9%** (+6.1%)	**+10.3** (+12.4)
Low, Direct, FPR=1.6	+0.5% (+1.0%)	+1.2% (Minimum)	+4.5% (+8.1%)	+11.5% (+5.1%)	+10.4 (+11.9)
High, Direct, FPR=1.6	+2.6% (+3.1%)	+3.9% (+3.7%)	+3.0% (+4.7%)	+6.9% (+5.9%)	+10.5 (+12.5)
Low, Direct, FPR=1.7	**Minimum** (Minimum)	**+2.8%** (+1.3%)	**+3.4%** (+1.2%)	**+18.9%** (+14.3%)	**+16.1** (+16.7)
High, Direct, FPR=1.7	+1.2% (+1.6%)	+4.5% (+4.4%)	+0.5% (Minimum)	+12.7% (+13.4%)	+15.8 (+17.1)

For ramp weight, the minimum case has not changed compared to the results from reference 2, but the ramp weight penalties of the other cases have been reduced. For example, previously the ramp weight penalty of the high work, geared fan, FPR=1.4 case was 7.3%, versus only 2.0% with the revised engine designs. As noted previously, the minimum block fuel case did change from the low work, direct drive, FPR=1.6 case to the high work, geared, FPR=1.5 case. The fuel consumption penalty of the FRP=1.4, geared engine case was greatly reduced from 5.9% to only 0.5%. The block NO_X penalty of the low FPR, geared designs was also greatly reduced, from 15.8% to only 2.7% at FPR=1.4. The minimum noise case continues to be the geared, FPR=1.4 case, but there is a slight reduction in the noise penalties of the other cases.

With improved performance of the low FPR engines resulting from the engine design changes implemented in this study, there is less of a trade-off between aircraft noise and fuel consumption than found previously in reference 2. In reference 2, pursuing minimum fuel consumption resulted in a 12 EPNdB penalty in cumulative noise, whereas pursuing minimum noise resulted in a 6% penalty in fuel consumption. For the current study, pursuing minimum fuel consumption (which now occurs at a lower FPR) only results in a 4 EPNdB penalty in noise and pursuing minimum noise only results in a 0.5% penalty in fuel consumption.

Which design is better overall depends, in part, on the relative value of low noise, low fuel consumption, and low NO_X emissions to the airlines, which in turn depends on external factors such as fuel cost, airport noise restrictions, and government regulations. Selecting a balanced engine design that performs well in all categories is somewhat subjective; however, the geared fan, high work, FPR=1.5 case seems to offer the best overall performance. It has relatively good weight, fuel consumption, noise, and emissions results. Bypass ratio for this engine is in the 14 range, at the lower end of what is usually considered "ultra-high bypass ratio." If noise were the dominant consideration, a lower FPR would offer reduced noise with small weight, fuel, and NO_X penalties. The emergence of a high work, geared, FPR=1.5 engine as the best balanced design is a function of the approach and assumptions in this study. Changes in engine or airframe design rules and technology assumptions could lead to a different result.

7.0 Concluding Remarks

A comprehensive exploration of the turbofan engine design space for an advanced technology single-aisle transport was previously documented in reference 2. Through the course of that study and in a subsequent evaluation of the approach and results, a number of enhancements to the engine design ground rules and assumptions were identified. A follow-on effort was initiated to investigate the impacts of these changes on the study results.

The fundamental conclusions of the prior study have not changed with the changes to the engine designs. With the ground rules, architectures, and assumptions used in this study: empty weight and ramp weight (often surrogate indicators of cost) are minimized with high FPR; block fuel consumption is minimized with a FPR of 1.5-1.6; block NO_X emissions are minimized with high FPR; and LTO NO_X and certification noise are minimized with FPR as low as possible. The best compromise FPR appears to be ~1.5, having good performance across all the metrics of interest (ramp weight, fuel consumption, emissions, and noise). Relative to 1998 EIS technology, the advanced configurations have the potential for significant benefits: up to 29% reduction in fuel consumption, 50-60% reductions in NO_X emissions, and greater than 25 EPNdB cumulative noise reduction.

The engine design changes did change the relative performance of direct drive and geared fan engines and the fuel consumption and weight penalties of low FPR. Because of a relative improvement in the geared fan cases, the point at which gearing becomes beneficial moved to higher FPR. In the previous study, the high work, geared fan and low work, direct drive fan FPR=1.5 engines resulted in similar aircraft characteristics. In the current study, the FPR=1.5 geared fan engine is noticeably better than the low work, direct drive engine at that FPR. The primary reasons for this shift are the higher relative weights of the low work, direct drive engines and the elimination of unnecessary penalties on the high work engines caused by the previous LPT cooling philosophy. Even though the engine design changes did not change the optimum FPR for each of the metrics for a given engine architecture, it did change the penalties associated with being away from that optimum. In particular, the penalties of low FPR were reduced significantly for the high work, geared fan architecture. This enables lower FPR (and correspondingly lower aircraft noise) to be implemented with a minimal fuel consumption penalty.

8.0 References

1. Wall, R,; Kingsley-Jones, M.; Norris, G.; Mecham, M.; Warwick, G.; and Shannon, D.: *Leap of Faith – Cseries killer or not, Airbus launches A320NEO but keeps an eye on what is next.* Aviation Week & Space Technology, December 6, 2010. pp. 24-28.

2. Guynn, M. D.; Berton, J. J.; Fisher, K. L.; Haller, W. J.; Tong, M. T.; and Thurman, D. R.: *Engine Concept Study for an Advanced Single-Aisle Transport*. NASA TM-2009-215784, August 2009.

3. Lytle, J.K.: *The Numerical Propulsion System Simulation: An Overview*. NASA TM-2000-209915, June 2000.

4. NPSS User Guide Software Release: NPSS_1.6.3 AL.

5. NPSS Reference Sheets Software Release: NPSS_1.6.3 AL.

6. Onat, E.; and Klees, G.: *A Method to Estimate Weight and Dimensions of Large and Small Gas Turbine Engines.* NASA CR 159481, 1979.

7. Tong, M.T.; Halliwell, I.; Ghosn, L.J.: *A Computer Code for Gas Turbine Engine Weight and Life Estimation*, ASME Journal of Engineering for Gas Turbine and Power, volume 126, no. 2, April 2004.

8. Tong, M.T.; Naylor, B.A.: *An Object-Oriented Computer Code for Aircraft Engine Weight Estimation*, GT2008-50062, ASME Turbo-Expo 2008, June 9-13, 2008.

9. Engine Comparison. http://www.aviationweek.com/media/images/awst_images/large/Leap-X_PW1000G.html. Accessed 7/30/2010.

10. McCullers, L.: *Aircraft Configuration Optimization Including Optimized Flight Profiles*. Proceedings of the Symposium on Recent Experiences in Multidisciplinary Analysis and Optimization, NASA CP 2327, April 1984.

11. Ardema, M. D.; Chambers, M. C.; Patron, A. P; Hahn, A. S.; Miura, H.; and Moore, M. D.: *Analytical Fuselage and Wing Weight Estimation of Transport Aircraft*. NASA TM 110392, May 1996.

12. 787 Dreamliner Program Fact Sheet. http://www.boeing.com/commercial/787family/programfacts.html. Accessed 4/9/2007.

13. 737-800 Technical Characteristics. http://www.boeing.com/commercial/737family/pf/pf_800tech.html. Accessed 4/9/2007.

14. Gillian, Ronnie E.: *Aircraft Noise Prediction Program User's Manual*. NASA TM-84486, 1983.

15. Zorumski, William E.: *Aircraft Noise Prediction Program Theoretical Manual*. NASA TM-83199, 1981, Parts 1 and 2 (Currently maintained at NASA LaRC by the ANOPP team in electronic format and provided upon request; Latest revision: December 2005).

16. Code of Federal Regulations, Title 14, Chapter I, Part 36. *Noise standards: Aircraft type and airworthiness certification.*

17. Stone, J.R.; Krejsa, E.A.; Clark, B.J.; and Berton, J.J.: *Jet Noise Modeling for Suppressed and Unsuppressed Aircraft in Simulated Flight.* NASA TM-2009-215524, 2009.

18. Janardan, B.A.; Hoff, G.E.; Barter, J.W.; Martens, S.; Gliebe, P.R.; Mengle, V.; and Dalton, W.N.: *AST Critical Propulsion and Noise Reduction Technologies for Future Commercial Subsonic Engines – Separate-Flow Exhaust System Noise Reduction Evaluation*. Final Report: NAS3–27720, Area of Interest 14.3, General Electric Report R98AEB152, May 1998.

19. Neubert, R.; Bock, L.; Malmborg, E.; and Owen-Peer, W.: *Advanced Low Noise Research Fan Stage Design*. NASA CR 97-206308, 1997.

20. Sutliff, D.L.; Jones, M.G.; Hartley, T.C.: *Attenuation of FJ44 Turbofan Engine Noise with a Foam-Metal Liner Installed Over-the-Rotor*. 15th AIAA/CEAS Aeroacoustics Conference, AIAA-2009-3141, 2009.

21. Jones, M.; Parrott, T.; Sutliff, D.; Hughes, C.: *Assessment of Soft Vane and Metal Foam Engine Noise Reduction Concepts*. 15th AIAA/CEAS Aeroacoustics Conference, AIAA-2009-3142, 2009.

22. Code of Federal Regulations, Title 14, Chapter I, Part 34. *Fuel Venting and Exhaust Emission Requirements for Turbine Engine Powered Airplanes.*

REPORT DOCUMENTATION PAGE	*Form Approved* *OMB No. 0704-0188*

1. REPORT DATE *(DD-MM-YYYY)*	**2. REPORT TYPE**	**3. DATES COVERED** *(From - To)*
01- 01 - 2011	Technical Memorandum	

4. TITLE AND SUBTITLE
Refined Exploration of Turbofan Design Options for an Advanced Single-Aisle Transport

5a. CONTRACT NUMBER

5b. GRANT NUMBER

5c. PROGRAM ELEMENT NUMBER

6. AUTHOR(S)
Guynn, Mark D.; Berton, Jeffrey J.; Fisher, Kenneth L.; Haller, William J.; Tong, Michael T.; Thurman, Douglas R,

5d. PROJECT NUMBER

5e. TASK NUMBER

5f. WORK UNIT NUMBER
561581.02.08.07.13.11

7. PERFORMING ORGANIZATION NAME(S) AND ADDRESS(ES)
NASA Langley Research Center
Hampton, VA 23681-2199

8. PERFORMING ORGANIZATION REPORT NUMBER
L-19970

9. SPONSORING/MONITORING AGENCY NAME(S) AND ADDRESS(ES)
National Aeronautics and Space Administration
Washington, DC 20546-0001

10. SPONSOR/MONITOR'S ACRONYM(S)
NASA

11. SPONSOR/MONITOR'S REPORT NUMBER(S)
NASA/TM-2011-216883

12. DISTRIBUTION/AVAILABILITY STATEMENT
Unclassified - Unlimited
Subject Category 01
Availability: NASA CASI (443) 757-5802

13. SUPPLEMENTARY NOTES

14. ABSTRACT
A comprehensive exploration of the turbofan engine design space for an advanced technology single-aisle transport (737/A320 class aircraft) was conducted previously by the authors and is documented in a prior report. Through the course of that study and in a subsequent evaluation of the approach and results, a number of enhancements to the engine design ground rules and assumptions were identified. A follow-on effort was initiated to investigate the impacts of these changes on the original study results. The fundamental conclusions of the prior study were found to still be valid with the revised engine designs. The most significant impact of the design changes was a reduction in the aircraft weight and block fuel penalties incurred with low fan pressure ratio, ultra-high bypass ratio designs. This enables lower noise levels to be pursued (through lower fan pressure ratio) with minor negative impacts on aircraft weight and fuel efficiency. Regardless of the engine design selected, the results of this study indicate the potential for the advanced aircraft to realize substantial improvements in fuel efficiency, emissions, and noise compared to the current vehicles in this size class.

15. SUBJECT TERMS
Aircraft Design; Aircraft Noise; Engine Airframe Integration; Engine Design; Propulsion System Performance; Turbofan Engines

16. SECURITY CLASSIFICATION OF:			**17. LIMITATION OF ABSTRACT**	**18. NUMBER OF PAGES**	**19a. NAME OF RESPONSIBLE PERSON**
a. REPORT	**b. ABSTRACT**	**c. THIS PAGE**			STI Help Desk (email: help@sti.nasa.gov)
					19b. TELEPHONE NUMBER *(Include area code)*
U	U	U	UU	36	(443) 757-5802